Materials Science & Engineering A 597 (2014) 295–303

Contents lists available at ScienceDirect

Materials Science & Engineering A

journal homepage: www.elsevier.com/locate/msea

Annealing twin development during recrystallization and grain growth in pure nickel

Y. Jin [a,*], B. Lin [b], M. Bernacki [a], G.S. Rohrer [b], A.D. Rollett [b], N. Bozzolo [a]

[a] MINES ParisTech, CEMEF – Centre de Mise en Forme des Matériaux, CNRS UMR 7635, BP 207, 1 rue Claude Daunesse, 06904 Sophia Antipolis cedex, France
[b] Carnegie Mellon University, 5000 Forbes Avenue, Pittsburgh 15213, USA

ARTICLE INFO

Article history:
Received 5 September 2013
Received in revised form
18 November 2013
Accepted 8 January 2014
Available online 17 January 2014

Keywords:
Annealing twin
Recrystallization
Grain growth
In situ annealing
EBSD

ABSTRACT

A 99.995% pure Ni sample, compressed to 25%, was annealed in a SEM chamber and changes in the density of annealing twins were monitored in situ during recrystallization and grain growth. In addition to average microstructural measurements, the evolution of individual grains was also observed. Both the average annealing twin density in the recrystallized domain and the annealing twin density per grain increased during recrystallization. The rate of increase in twin density correlates with the velocity of the recrystallization front. During grain growth, however, the average annealing twin density decreased. The in situ EBSD observations showed both the formation of new twins and the extension of existing twins during annealing. The observations reported here suggest that the existing models for annealing twin formation are incomplete.

1. Introduction

In 1926, Carpenter and Tamura [1] reported on annealing twin formation and annealing twins were commonly mentioned in articles containing metallography before this. Since then, annealing twins have been observed in almost all deformed and subsequently annealed F.C.C. metals except for aluminum.

Annealing twin boundaries affect many properties such as corrosion and fatigue resistance in a large variety of materials [2] because of their low energy [3]. Annealing twin boundaries, especially coherent twin boundaries, are fundamental for 'Grain Boundary Engineering' [4–6]. Even today metallurgists still do not agree on the mechanism of their formation.

There are four schools of thought on annealing twin formation: (i) the grain encounter model [7–9], (ii) the stacking fault model [10] where stacking fault packets formed during grain boundary migration generate annealing twins [11], (iii) the grain boundary dissociation model [11–13] which involves a general high angle boundary dissociating into a coherent twin boundary, an incoherent twin boundary and a low energy boundary to decrease the overall interfacial energy, and (iv) the growth accident model [1,14–17]. The growth accident model, which asserts that a coherent twin boundary forms at a migrating grain boundary because of a stacking error, is supported by a majority of recent experimental results [18–21].

In the growth accident model, the grain boundary migration distance and the grain boundary migration velocity are two key factors promoting the generation of annealing twins. Gleiter [14] and Pande [15] derived models for predicting annealing twin density which are consistent with this idea. Gleiter's formulation was shown to be capable of accurately determining the annealing twin density [19]. The effect of prior deformation was introduced into Pande's model [21] but this and other prior work has mainly focused on the average annealing twin density evolution in the grain growth regime. The purpose of this work is to analyze annealing twin formation in individual grains during recrystallization and to quantify annealing twins during both recrystallization and grain growth. We present evidence that the annealing twin density increases during recrystallization, but decreases during grain growth.

2. Experimental details

Commercially pure nickel (99.995 wt%) was used in this experiment. A cylindrical sample, 5 mm in diameter and 3 mm in height, was first compressed at room temperature to a 25% height reduction. After deformation, the sample was metallographically prepared with a final mechanical polish using a 0.5 μm colloidal SiO_2 suspension and a 200 μm thick slice was extracted for study. The sample was annealed in situ at 400 °C in a FEI XL30 ESEM microscope equipped with a TSL EBSD system. The heating device was a thin tantalum foil on which the sample was spot-welded [22], which allows to achieve very high heating and cooling rates (100 °C/s) and enables precise control of short annealing times. EBSD orientation maps were recorded with a 0.5 μm step size to

* Corresponding author. Tel.: +33(0)493678924; fax: +33(0)492389752.
E-mail address: yuan.jin@mines-paristech.fr (Y. Jin).

0921-5093/$ - see front matter © 2014 Elsevier B.V. All rights reserved.
http://dx.doi.org/10.1016/j.msea.2014.01.018

compromise between spatial resolution and acquisition time. To capture the initial stages of the recrystallization regime, short annealing times (2 s) were used at the start of the experiment. The heat treatment sequence is detailed in Fig. 1. The OIM™ software was used to analyze the EBSD data. The influence of sample thickness on grain boundary migration was not considered here. Annealing twin density, defined as the number of twin boundary intercepts per unit length, was calculated using Eq. (1) [23],

$$\text{Twin density} = \frac{L_{tb}}{S}\frac{2}{\pi}, \quad (1)$$

where L_{tb} is the twin boundary length and S is the corresponding area. Note that measuring intercepts are not relevant for evaluating twin boundaries inside recrystallizing grains only and therefore lengths of twin boundaries detected inside the recrystallized grains provided the basis for the results reported here. Also, all Σ3 boundaries are included in order to avoid the uncertainty associated with estimating whether any given boundary segment is a coherent or incoherent twin.

Following typical practice, the recrystallized grains were defined in the EBSD maps by a criterion that the Grain Orientation Spread (GOS) was less than 1° [24]. GOS is defined as the average of the misorientation between the orientation of each point inside a grain and the average orientation of that grain. For grain detection, the minimum misorientation angle to define a grain boundary was set to 5° and twins were ignored. Additionally, isolated pixels were not considered as grains. No additional clean up was performed.

3. Experimental results

3.1. Recrystallization

The series of EBSD maps in Fig. 2 illustrates the microstructural development during recrystallization. The white lines mark the annealing twin boundaries, which are defined by a misorientation of 60° about the ⟨111⟩ axis with a tolerance of 8.66°, according to Brandon's criterion [25].

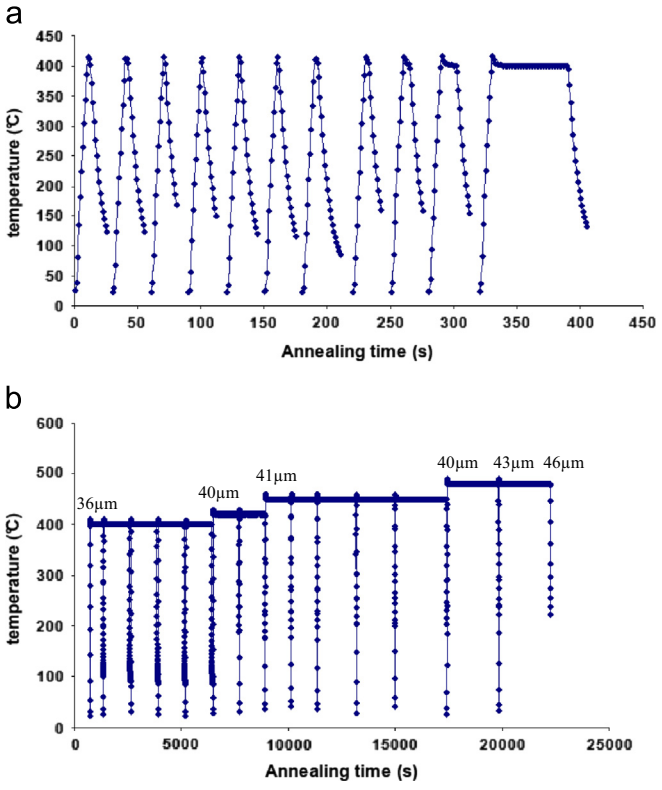

Fig. 1. In situ heat treatment sequence for the (a) recrystallization and (b) grain growth regimes. The area average grain sizes corresponding the main annealing steps are indicated.

The first map, recorded before the heat treatment, shows the heterogeneity of deformation. Recrystallizing grains first appeared and grew rapidly in the most deformed areas where the quality of Kikuchi patterns were initially low (Fig. 3), and accordingly the reliable-indexing rate was low. The Kikuchi pattern quality index map suggests the existence of deformation substructures in the form of submicron cells. Unfortunately, those cells are not well resolved under the acquisition settings that were used and the indexing reliability in those regions is too poor to analyze precisely the local crystallographic texture of the highly deformed areas and relate it to the orientations of the new grains. In addition it is worth mentioning that new grains may nucleate below the observed surface. For both reasons, the influence of the deformation substructures on recrystallization and twin generation was not analyzed at this small scale. As recrystallization progressed, the first recrystallization nuclei grew together and formed clusters while new grains continued to appear in less deformed areas. The recrystallized grains and grain clusters began to impinge before the end of recrystallization. The overall recrystallization kinetics is illustrated in Fig. 4. In the early stages, the recrystallization nuclei grew independently and the recrystallization fraction increased rapidly. As impingement occurred, the recrystallized grains formed clusters, and recrystallization fronts migrated at the rim of the clusters only, effectively reducing the transformation rate. The incubation time for recrystallization was negligible in this case.

3.1.1. Annealing twin density evolution in individual grains during recrystallization

For the purpose of tracking the evolution of individual grains, four recrystallized grains (colored red in Fig. 5) were selected. Annealing twins were generated very early in the recrystallization process. As the recrystallized grains grew into the deformed matrix, new annealing twins were generated (see Fig. 5). However, after impingement of the recrystallized grains, far fewer annealing twins were generated.

The change in the size (equivalent circle diameter) of the four sampled grains with time is described in Fig. 6(a). Despite their different size ranges, the individual grains exhibit the same trend of first increasing in size and then stagnating before the end of recrystallization. The annealing twin density per grain was calculated with Eq. (1) with the twin boundary length in the grain and the area of the grain at each of the annealing steps (Fig. 6(b)).

The twin densities in the first three selected grains exhibit a non-linear relationship with the equivalent circle diameters (Fig. 6(c)). More precisely, the twin density increased most rapidly at the beginning of recrystallization and the rate of increase decreased monotonically with increasing recrystallized fraction. Meanwhile, the twin density in the fourth individual grain seems to exhibit a different trend from the others in that the twin density increased rapidly until the end of recrystallization. The reasons for this are shown by the small circles on Fig. 5 (grain 4 after 18 s annealing). The small grain in the yellow circle forms a twin boundary with grain 4, only visible after 90 s annealing. In the blue circle the short annealing twin boundaries already existing after 18 s extend as the recrystallization front migrates into the deformed matrix. These two local phenomena increased the annealing twin density in the fourth grain without resulting in a significant increase in grain size. Such local events are responsible for the sharp increase in annealing twin density in the fourth grain till the end of recrystallization in Fig. 6(c).

Fig. 7 shows the rate of increase of annealing twin density, i.e. the slope of Fig. 6(b), as a function of the growth rate of